1-1-2015

Effective tuning of bimetallic composition of gold-copper nanomolecules and the emergence of plasmon-like feature in optical spectra

Asantha Champika Dharmaratne
University of Mississippi

EFFECTIVE TUNING OF BIMETALLIC COMPOSITION OF GOLD-COPPER NANOMOLECULES AND THE EMERGENCE OF PLASMON-LIKE FEATURE IN OPTICAL SPECTRA

Asantha C. Dharmaratne

A thesis submitted in partial fulfillment
of the requirements for the degree of

Master of Science
Department of Chemistry and Biochemistry

University of Mississippi

May 2015

ABSTRACT

$Au_{144-x}Cu_x(SR)_{60}$ alloy nanomolecules were synthesized and characterized by using ESI-MS to atomic precision. A maximum of 23 copper atoms replace the gold atoms; when the number of copper atoms is higher than eight, a surface plasmon-like peak appears at ~520 nm. Based on the fundamental, elemental properties of Au and Cu, we predict a mixed atomic ordering and incorporation into the Au_{12} and Au_{42} shells of the proposed icosahedral structured model. Alloy nanomolecules reported here could have potential applications in the field of catalysis and optical sensors.

ACKNOWLEDGEMENTS

I would like to thank Dr. Amala Dass for his support toward my research. His guidance and motivation from the beginning has helped me accomplish numerous achievements which include awards, peer-reviewed publications, and more. I would also like to thank all the graduate students and undergraduate students in the Dass's group. Along with the faculty and staff at the department of chemistry and biochemistry for their immense support. Additionally, I would like to thank my research committee, Dr. Steven R. Davis and Dr. James Cizdziel. This work has been supported, in part, by the National Science Foundation, as well as the University of Mississippi.

LIST OF ABBREVIATIONS

SR	A thiol group or a thiolate ligand
UV-vis-NIR	Ultraviolet-visible-Near Infrared
MS	Mass spectrometry
MALDI-TOF	Matrix-Assisted Laser Desorption/ Ionization- Time of Flight
ESI	Electrospray Ionization
Au	Gold
Cu	Copper
SEC	Size Exclusion Chromatography
THF	Tetrahydrofuran
BHT	Butylated hydroxytoluene
amu	atomic mass unit

LIST OF FIGURES

TABLE OF CONTENTS

CHAPTER 1: INTRODUCTION TO NANOPARTICLES

WHAT ARE NANOMOLECULES?

By definition, particles with a diameter ranging from 1 nm to 100 nm are known as nanomolecules. These nanomolecules have a fixed composition that can be characterized by mass spectrometry. More specifically, when these particles are smaller than 3nm they are known as ultra-small nanomolecules. The history of gold nanoparticles dates back to the mid nineteenth century; and in 1857, Michael Faraday prepared a colloidal gold sample by reducing gold salt with phosphorous.[1] Gold and alloy ultra-small nanoparticles are of particular interest because they have a precise number of gold atoms and thiolate ligands, which gives them unique characteristics. One of these characteristics being their definitive absorption shift with size.

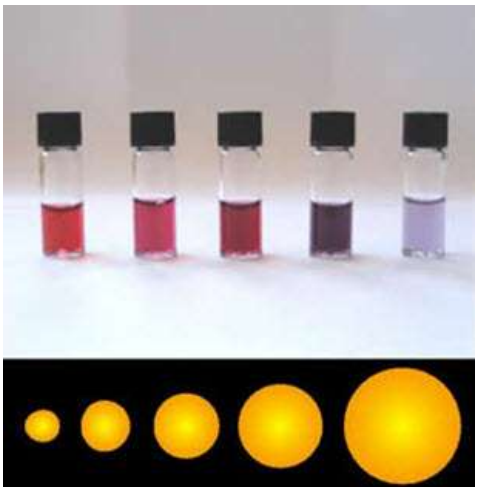

Figure 1. The color of gold colloidal change with the size of the gold nanoparticle

These nanoparticles have size dependent electronic properties that have been identified with UV-vis NIR spectroscopy. this is the reason, ultra small nanoparticles possess molecular like properties. As shown in Figure 1. The optical properties of the nanoparticles change with size.

Furthermore, these gold nanoparticles absorb light at different wavelengths depending on their diameter due to their size dependent surface plasmon resonance frequency.[2] This phenomenon explains why gold nanoparticles illustrate beautiful colors when exposed to light. Another example of this phenomenon, is the Lycurgus cup which is known to be one of the outstanding accomplishments of the ancient glass industry because of these unusual optical effects displayed by the glass.[3]

Figure 2. The Lycurgus Cup represents one of the outstanding achievements of the ancient glass industry

THE STRUCTURES OF GOLD NANOMOLECULES

The crystal structure of $Au_{25}(SR)_{18}$

The stability a nanomolecule often depends its geometrical structure. Therefore, an in-depth explanation on how the atoms have arranged in a thiolate protected gold nanomolecule is required. The basic structure of a thiolate protected gold nanomolecule is composed of an icosahedral metallic gold core, surrounded by thiolate ligands. The atomic arrangement of $Au_{25}(SR)_{18}$ is shown below in Figure 3, 13 out of 25 gold atoms are located in the icosahedron metallic core. The remaining 12 gold atoms are bound to the thiolate ligands. These thiolate ligands are referred to as staple motifs; each staple motif is composed of gold and sulfur atoms. The staple motifs can be categorized into two groups, long and short staples.[4]

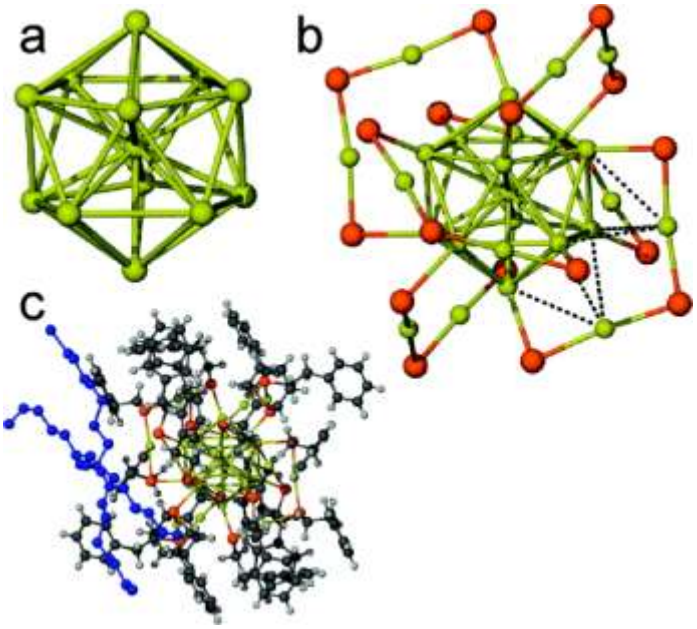

Figure 3. Atomic distribution and geometrical composition of $Au_{25}(SR)_{18}$ nanomolecule

For an example, a short staple motif contains a gold atom and two sulfur atoms in the following pattern of RS-Au-SR. Similarly, long staple motif contains two gold atoms and three sulfur atoms as shown above in Figure 3b.

The crystal structure of $Au_{144}(SR)_{60}$

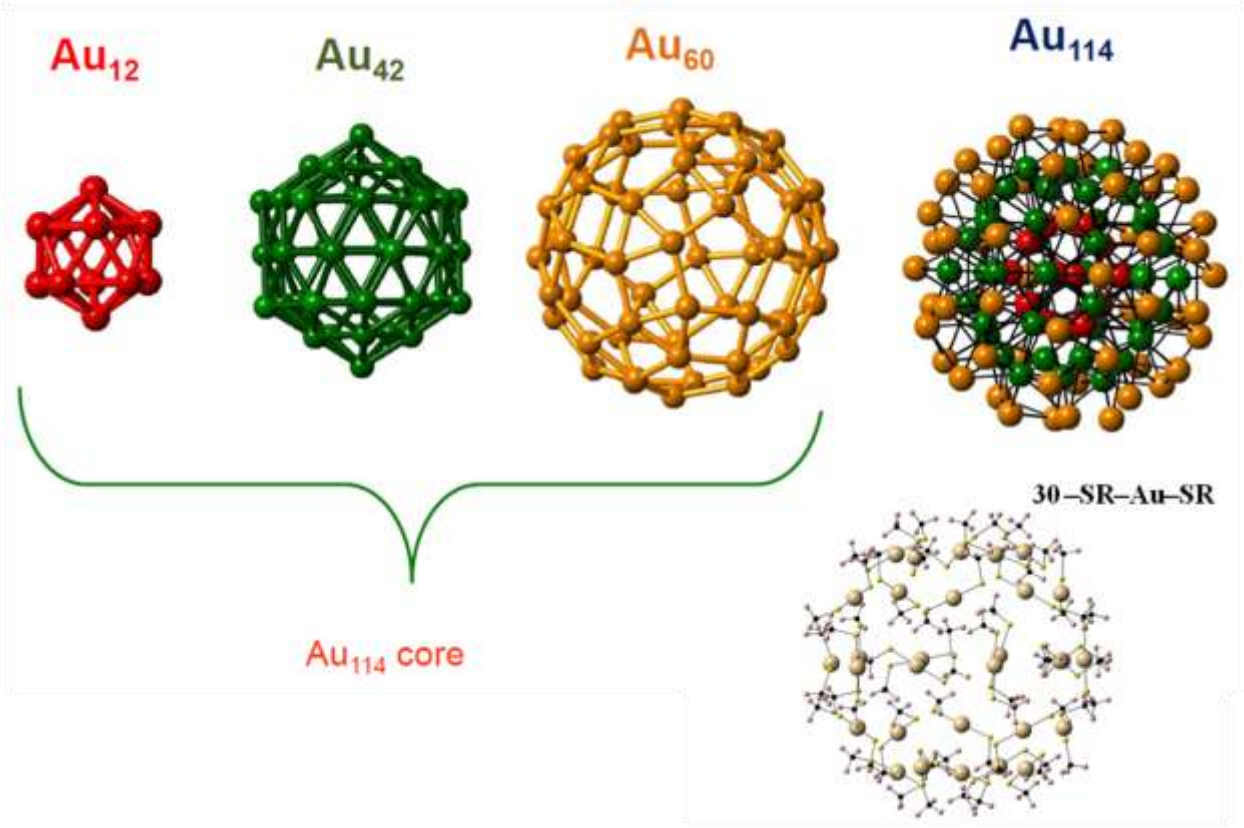

Figure 4. Atomic distribution and geometrical composition of $Au_{144}(SR)_{60}$ nanomolecule

The structure model for $Au_{144}(SR)_{60}$ has been proposed by theoretical calculations.[5] Similar, to the atomic arrangement of $Au_{25}(SR)_{18}$, $Au_{144}(SR)_{60}$ has a hollow icosahedron gold metallic core

comprised with 12 atoms. The central hollow metallic core is shown in Au_{12} (red) in Figure 4. Around the metallic core, there are two metallic gold shells containing 42 and 60 atoms respectively. These two metallic gold shells are labeled as Au_{42} (olive green) and Au_{60} (orange). The outermost shell is composed of staple motifs. Unlike in $Au_{25}(SR)_{18}$, the staple motifs in $Au_{144}(SR)_{60}$ has only one gold atom with two sulfur atoms per motif. In other words, the staple motifs of $Au_{144}(SR)_{60}$ can be considered as short staple motifs. As shown in Figure 4, there are 30 staple motifs bonded to the Au_{60} metallic shell. There are 30 gold atoms and 60 sulfur atoms in the staple motifs (30 x RS-Au-SR). As shown in Figure 4, there are 144 gold atom and 60 sulfur atoms (thiolate ligands), 114 of the gold atoms compose the metallic core, the remaining 30 gold and 60 sulfur atom create the staple motifis.

CHAPTER 2: $Au_{144-x}Cu_X(SC_6H_{13})_{60}$ NANOMOLECULES: EFFECT OF Cu INCORPORATION ON COMPOSITION AND PLASMON-LIKE PEAK EMERGENCE IN OPTICAL SPECTRA

INTRODUCTION

Nanomolecules have potential applications in catalysis,[6] sensors,[7] energy sources[8] and in the medical field. The properties of metal nanoparticles including stability, electronic and geometric structure, can be tuned by doping with other metals to form nanoalloys.[9] Copper doping with gold to form thiolate protected gold-copper nanoalloys drastically changes the electronic structure and catalytic properties, when compared with monometallic gold nanoparticles.[10] Copper nanoparticles are used as industrial catalysts for CH_3OH synthesis, CO_2 reduction, CO oxidation. But, copper has the tendency to oxidize readily compared to other metals and compromise catalytic activity.[11] Gold, resistant towards corrosion and oxidation, has been used to form bimetallic nanoalloys in order to minimize the oxidation of copper.[12] Bracey et. al. report that catalysts produced from thiol-stabilized pre-formed AuCu alloy particles were ten times more active than those prepared by impregnation, in the process of propene oxidation.[13] Several bimetallic alloy nanomolecules including Au-Pd,[14-16] Au-Ag,[17-19] Au-Pt[20] are reported. Except for $Au_{25-x}Cu_x(SR)_{18}$ reported by Negishi group, no other thiolate protected gold nanomolecules have been doped with copper.[21,22] Au_{144} is one of the most stable nanomolecules[23] and the $Au_{144-x}Cu_x(SR)_{60}$ nanoalloy would be an ideal candidate for alloying.

RESEARCH METHODLOGY

Materials

Chemicals: phenylethanemercaptan (SAFC, ≥ 99%),1-hexanethiol (ALDRICH, 95%), sodium borohydride (Acros, 99%), ethanol (Acros, 99.5%), trans-2[3[(4tertbutyl)-2-methyl-2-propenylidene]malonoitrile (DCTB matrix) (Fluka ≥ 99%) were purchased from Aldrich. Other solvents including: methanol, toluene, acetonitrile, and acetone, were used from fisher as received.

Instruments

ESI-MS (Electrospray Ionization- mass spectrometry) spectra were acquired on Waters SYNAPT HDMS instrument. MALDI-TOF (Matrix assisted laser desorption ionization time-of-flight) mass spectra were obtained on a Bruker Autoflex 1 mass spectrometer in linear positive mode using nitrogen laser (337 nm) with DCTB as the matrix. Ultra violet-visible absorption spectra were recorded in THF on a Shimadzu UV-1601 instrument.

Synthetic protocol: Crude product synthesis

$Au_{144-x}Cu_x(SR)_{60}$ nanoalloys were synthesized using different Au:Cu incoming molar ratio starting from 1:0, 1:0.025, 1:0.10, 1:0.30 and 1:0.50. For example, the following procedure was used to synthesis Au: Cu-1:0.025 ratios. Initially, 0.00432 g (0.026 mmol) of $CuCl_2.2H_2O$ was dissolved in Ethyl alcohol (5 mL, absolute 99.5%). Tetraoctylammonium bromide (TOABr)

(0.2346 g/ 0.468 mmol was dissolved in Ethyl alcohol (15 mL, absolute 99.5%). $HAuCl_4.3H_2O$ (0.0512 g/ 0.13 mmol) was dissolved in Ethyl alcohol (5 mL, absolute 99.5%) Then reagents transferred into a 100 mL round bottom flask under fast stirring (~700 rpm). After 30 minutes, 1-hexanethiol (0.468 mmol /0.05757 mL) of was added under continuous stirring at ~700 rpm. During this step, the organosulfur compounds can be varied as shown in Figure 4. The reaction mixture turned colorless after ~10 minutes. After 1 hour, $NaBH_4$ (0.3783 g/ 10 mmol) was dissolved in 10 mL of Ethyl alcohol (absolute 99.5%) was added into the reaction mixture. The reaction was stopped after 2 hours afterwards, excess thiols and other byproducts were removed thorough methanol wash (3 times). Then final product was extracted by THF. Further etching and solvent fractionation were done in order to isolate $Au_{144-x}\ Cu_x(SR)_{60}$ nanomolecules in pure form.

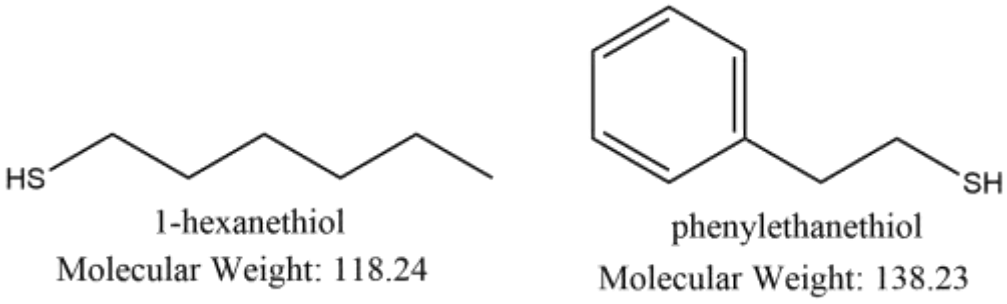

Figure 5. Thiolate ligands used to synthesize gold copper bimetallic nanomolecules

After obtaining the crude product from the initial synthesis, thermochemical treatment is essential to remove metastable clusters from the crude mixture. In the presence of these metastable clusters in a crude mixture would suppress the mass spectrometric signal of the molecule of interest during the analysis. Such metastable clusters can be removed by applying

harsh conditions to the crude mixture.[24] Harsh conditions are often considered as heating of the crude mixture at 80^0C with excess thiolate ligands (Figure 5.) under stirring. After subjecting the crude mixture to thermal chemical treatment for several hours (the time duration can be varied as needed), mass spectrometric analysis show the peak for the molecule of interest distinctively. As shown in the Figure 6, thermal chemical treatment process can be utilized to obtain either $Au_{25}(SR)_{18}$ or $Au_{144}(SR)_{60}$ from a mixture containing $Au_{25}(SR)_{18}$, $Au_{67}(SR)_{35}$, $Au_{102}(SR)_{44}$, and $Au_{144}(SR)_{60}$. This methodology also examines the stability of the synthesized product.

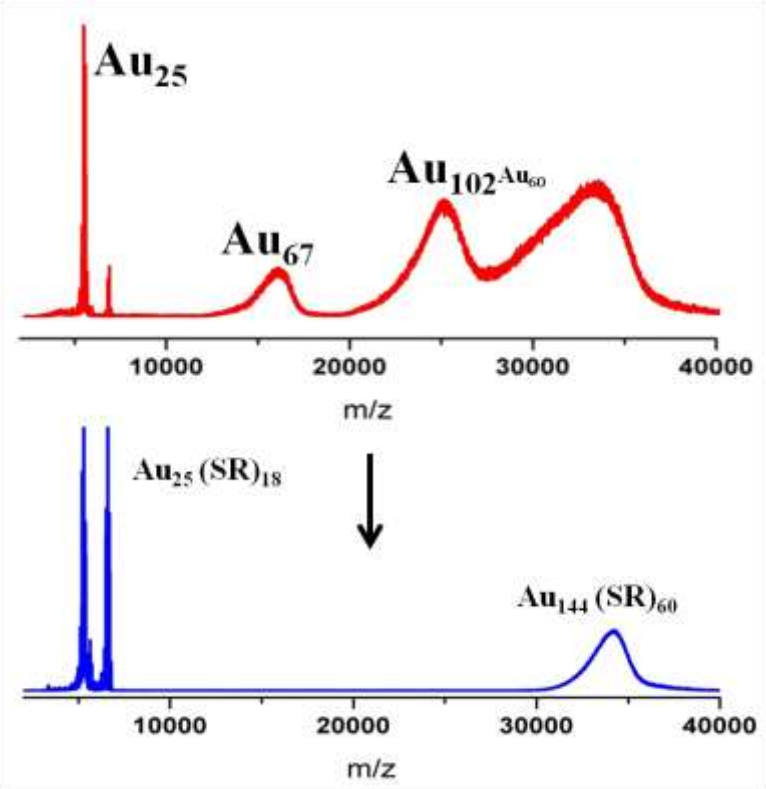

Figure 6. Before and after scenario of thermal chemical treatment process

Size exclusion chromatography (SEC)

The purification and separation of different gold nanomolecules can be achieved by adopting a technique called size exclusion chromatography. In this technique, gold nanomolecules travel through porous beads and elute at different time intervals based on the size of the nanomolecules in the mixture.[25] As depicted in Figure 6, smaller molecules travel through the porous beads while the larger molecules bypass it and elute. Since the smaller molecules travel through the beads, it takes more time to elute than the larger molecules. For that reason, SEC can be used as a technique to separate larger gold nanomolecules from smaller gold nanomolecules.

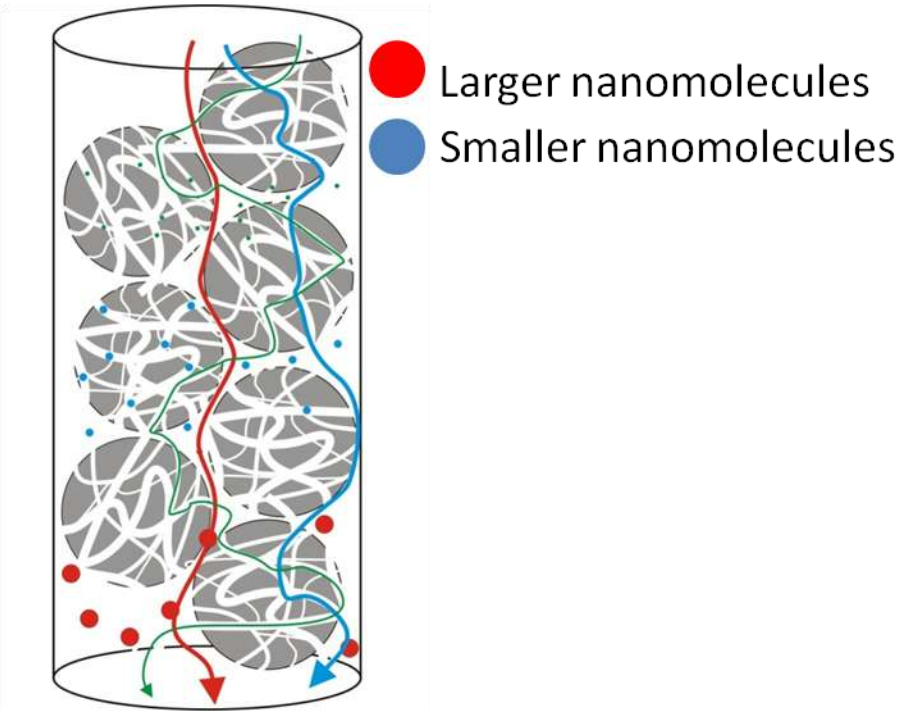

Figure 7. The pathway of large and small molecules through porous beads in SEC[26]

For an example, if the crude mixture in Figure 5 loaded on to an SEC column, initial fractions contain $Au_{144}(SR)_{60}$ and the later fractions contain $Au_{25}(SR)_{18}$. By adopting this methodology, an SEC column was prepared. A glass column packed with commercially available porous beads made out of polystyrene divinylbenzene after soaked in stabilized THF, with BHT as an inhibitor. The sample was then loaded on to the column after dissolving it in minimum amount of THF-BHT. It is important to have the eluent, THF-BHT and the column bed level together before loading the sample.[27] This method can be further developed by adjusting the column height or the surface area of the column bed in order to optimize the resolution as well as the separation of the molecules of interest. Figure 8 shows an actual SEC column and the fractions collected, that was performed in the Dass laboratory.

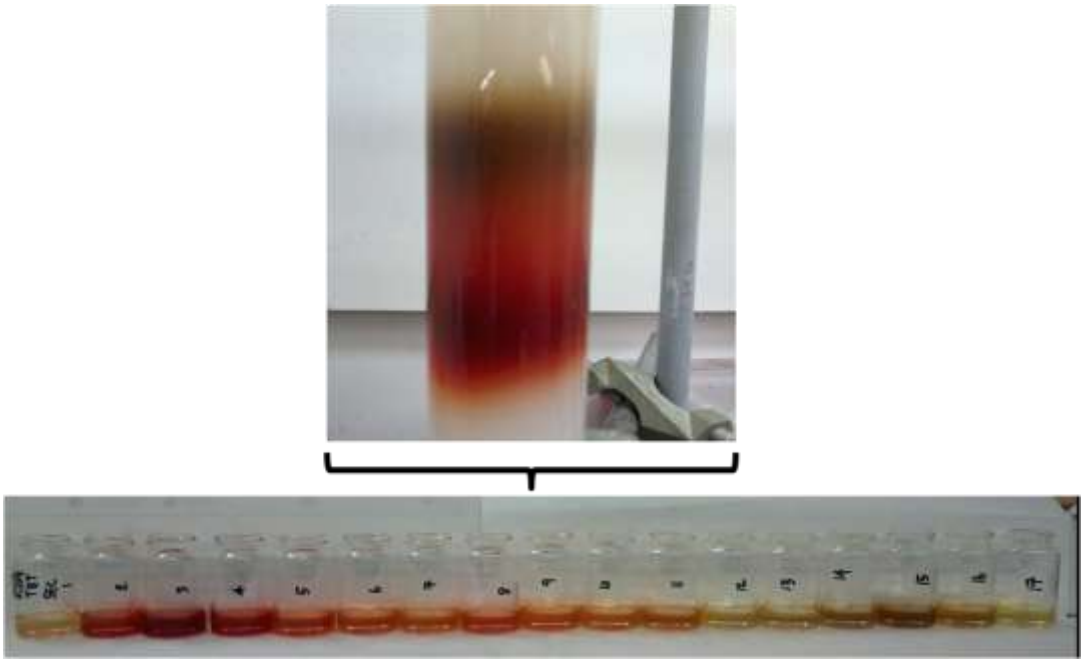

Figure 8. A series of samples collected from an SEC separation

CHAPTER 3: DATA ANALYSIS

MASS SPECTROMETRY

Mass spectrometric studies were performed by using MALDI TOF-MS- Bruker Daltonics Autoflex, JBL Scientific Voyager-DE Biospectrometry and ESI- Waters Synapts High Definition mass spectrometer. The identification of the gold nanomolecules was mainly carried out by these two mass spectrometric techniques. One of the advantages of these two types of mass spectrometric identification techniques is the amount of sample utilized for the analysis. From a highly diluted sample, it would only require 3 µL (MALDI TOF-MS) and 150 µL (ESI-MS) for the analysis. The molecular weight of $Au_{144}(SC_6H_{13})_{60}$ nanomolecule is 35,397 Da. MALDI-MS show broad peaks exclusively at ~35 kDa, which indicates absence of other species. On the other hand, ESI-MS generally shows high resolution peaks, due to the multiply charged peaks at lower mass.[28] The above figure shows MALDI and ESI-MS spectra of purified $Au_{144-x}Cu_x(SR)_{60}$ samples. MALDI-MS can be used to assess the purity of the sample.[29] ESI-MS spectra of the samples at different Au-Cu precursor ratios. The bottom spectra (in black) shows pure $Au_{144}(SC_6H_{13})_{60}$ at 35,397 m/z, with no Cu incorporation. When Cu is added in the synthetic mixture, with a $HAuCl_4$: $CuCl_2$ ratio of Au:Cu – 1:0.025, a maximum of 7 incorporations were observed, with the parent Au_{144} peak being the most intense one. The dotted lines are spaced at 67 m/z, indicative of successive Cu incorporations into $Au_{144}(SR)_{60}$. When the Au: Cu precursor ratio was increased to 1: 0.1, a maximum of 12 Cu atoms were incorporated. In addition to $Au_{144}(SC_6H_{13})_{60}$ peaks, there was another envelope of peaks of lower intensity, which will be discussed later. The envelope of peaks shows a Gaussian distribution with an average of 8 Cu atom incorporations. In the 1: 0.3 ratio, a maximum of 16 Cu atom incorporations were observed

with an average of 13 Cu atoms. But in this ratio, another set of peaks were observed within the $Au_{144-x}Cu_x(SR)_{60}$ envelope as discussed later. Upon increasing the ratio to Au:Cu- 1:0.5, an envelope of peaks with a maximum of 23 Cu atom incorporations were observed. When the ratio was increased further, no stable nanoparticles were obtained.

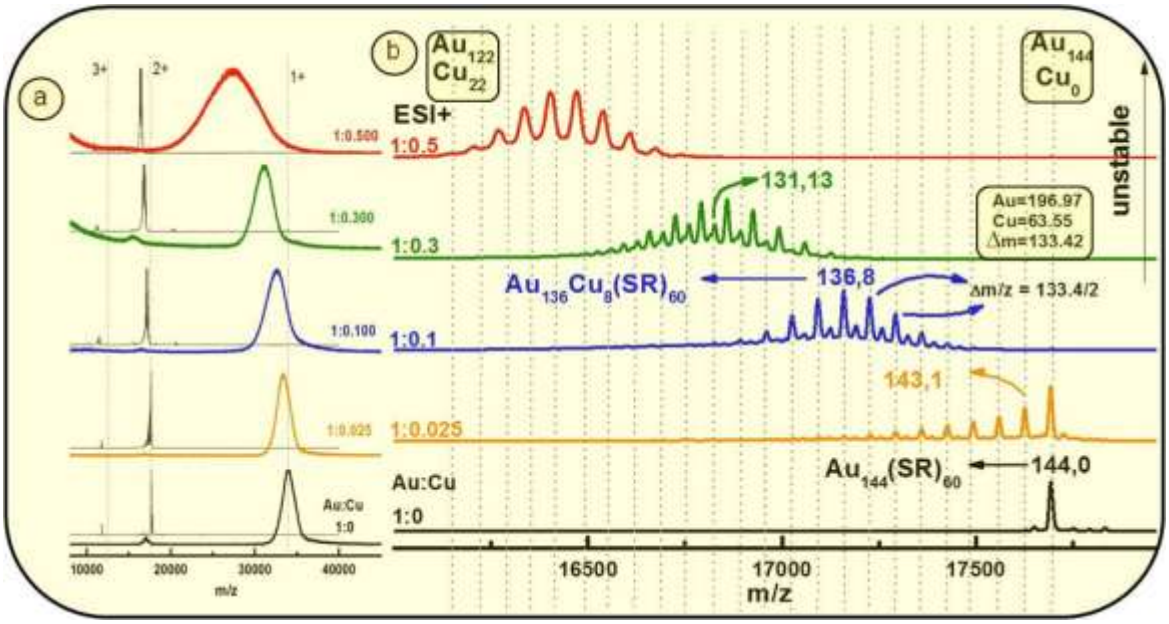

Figure 9. Compositional assignment using mass spectrometry.

The mass difference between the peaks in nanoalloys match up to the Au (196.97 Da) and Cu (63.55 Da) mass difference, $\Delta m = 133.42 /2$ m/z. The average number of Au and Cu atoms is denoted above each peak distribution. The black peak indicates $Au_{144}Cu_0(SR)_{60}$, and each dotted line to the left indicates a peak corresponding to one Cu atom doping. A maximum of 22 Cu atom incorporation was observed for the 1:0.5 ratio, above, which the nanomolecules are not stable.

ULTRA VIOLET VISIBLE SPECTROSCOPY

Optical and electronic properties of nanoalloys can be studied by UV-vis-NIR spectroscopy. For the investigation of such properties of gold copper bimetallic nanomolecules, the following instruments were used; Cary series UV-Vis NIR spectrophotometer and UV 1601 Shimadzu spectrophotometer. Figure 2 shows the UV-vis-NIR spectra of the pure $Au_{144-x}Cu_x(SR)_{60}$ sample. $Au_{144}(SR)_{60}$ (black curve) shows a monotonous curve, with minor bumps at ~520 nm and ~700 nm. At 1:0.025 ratio, the spectral (black curve) features from the monometallic $Au_{144}(SR)_{60}$ are diminished and appears a monotonous curve with no spectral (brown curve) features. When the Au:Cu ratio was increased to 1: 0.1, the spectrum (blue curve) shows a SPR-like broad peak/ band around 520 nm. Also, the 1: 0.3 and 1: 0.5 Au: Cu ratios show similar SPR peaks around 520 nm. Gold and copper show a surface plasmon resonance at ~520 nm and 550 – 600 nm respectively.[30,31] Based on that reasoning, the emergence of the SPR like peak at 520 nm could be an effect of gold. The emergence of plasmon like characteristics of the nanomolecule been observed after the precursor ratio of 1:0.025, Au: Cu. The changes in the electronic properties resemble a modulation in the electronic structure. These plasmon like changes, after the precursor ratio of 1: 0.025 could be due to a possible electronic structure modulation upon a certain number of copper atom incorporations.

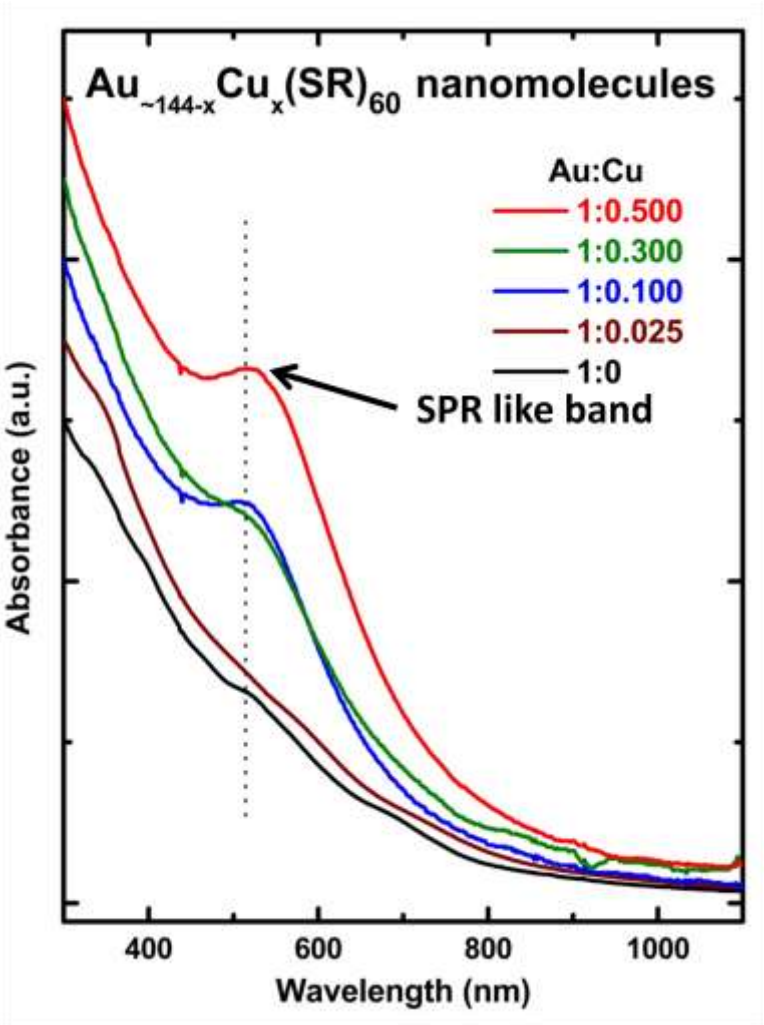

Figure 10. UV-visible absorption spectra of the $Au_xCu_y(SC_6H_{13})_z$ nanomolecules.

CHAPTER 4: RESULTS AND DISCUSSION

THEORETICAL RESULTS AND DISCUSSION

Recently, a structure model was proposed for $Au_{144}(SR)_{60}$ nanomolecule based on theoretical calculations.[5] The model comprises of a) an inner 12-atom icosahedral core (Au_{12}), surrounded by b) a second 42-atom (Au_{42}) shell, covered by c) an outer 60-atom shell (Au_{60}). Overall, the core is composed of three concentric shells, Au_{12}, Au_{42}, and Au_{60} accounting for 114 gold atoms. The remaining 30 gold atoms and 60 ligands are arranged in the form of 30 SR-Au-SR- short staples around the metallic core. To tune the properties of alloy nanomolecules, it is important to understand the location of metal atoms within the structure and the atomic ordering.

Figure 11 shows four examples of possible mixing patterns in bimetallic clusters, using two types of metal atoms, A (red) and B (yellow). Figure 11.a, depicts a possible core-shell segregation that would result from higher monometallic bond strengths from either atom, A or B. For instance, if A-A has a higher bond strength compared to B-B, then the core would be composed with type A atoms while the shell would be composed of type B atoms. Due to higher bond strengths of A-A, the interaction between type A atoms are greater than the interaction between type A and type B atoms, A-B. Figure 11.b shows an example of sub-cluster segregation. During sub-cluster segregation, a partial interaction between the two atoms takes place. This partial interaction forms an interface between the two types of atoms. Depending on the strength of the interaction, the number of A-B bond would be varied. Figure 11.b (left) is an example of where the A-B interactions are greater, meaning there are more A-B bonds at the interface. Similarly, when the A-B interactions are at minimal, the number of A-B bonds at the interface decreases as shown in Figure 11.b (right). When A-B bond strengths are greater than

the monometallic bonds of either metal results in mixed A-B nanoalloys. Such mixing can be found either ordered (left) or random (right) as shown in Figure 11.c. The fourth pattern, is similar to the core-shell segregation but with alternating A-B-A or A-B-A-B.

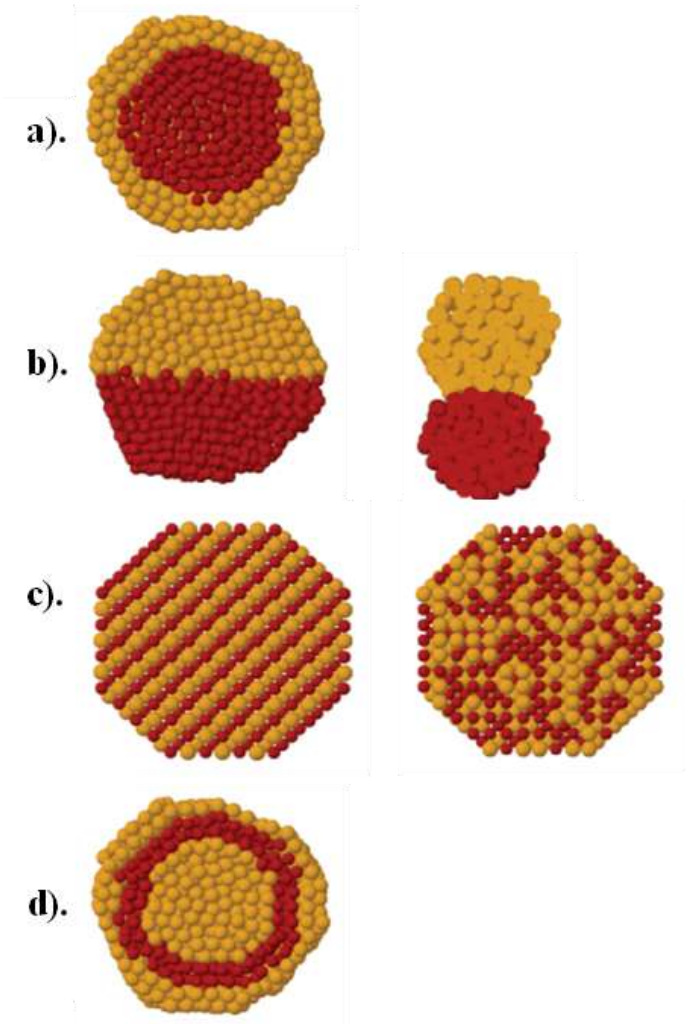

Figure 11. An illustration of possible mixing patterns of bimetallic clusters

The fundamental elemental properties of Au and Cu can be used to predict the arrangement of Au and Cu atoms in the nanoalloys.[9,12,32-36] Cerbelaud et al reports that Au_7Cu_{23}, $Au_{15}Cu_{15}$ and $Au_{23}Cu_7$ are the most stable homotops that can be found at the Gupta level for pyramidal clusters of composition[37, 38]. Previous studies done by Lorderito et al., Hsu et al., Rodrigues et al., and Wilson et al report a similar trend in free AuCu clusters.[35,36,39] The bond dissociation energies of Au-Cu (232 kJ/mol) > Au-Au (221 kJ/mol) > Cu-Cu (202 kJ/mol) suggests that the Au-Cu heteronuclear atomic bond is the strongest.[40] Such strong heteronuclear atomic bonds favor *mixing* of the two metal atoms instead of segregated or core-shell type atomic ordering.[9] Based on this, we propose mixing of Au-Cu atoms in $Au_{144-x}Cu_x(SR)_{60}$. In addition, when the Cu atoms are spread out between both Au_{12} and Au_{42} shells, the Au-Cu interactions are at their maximum. As the Au-Cu bond is the strongest, such interactions would render greater stability to $Au_{144-x}Cu_x(SR)_{60}$ alloys. Therefore, we propose a mixing of Au-Cu atoms, where the Cu atoms are incorporated into the Au_{12} and Au_{42} shells within the core (see scheme 1).

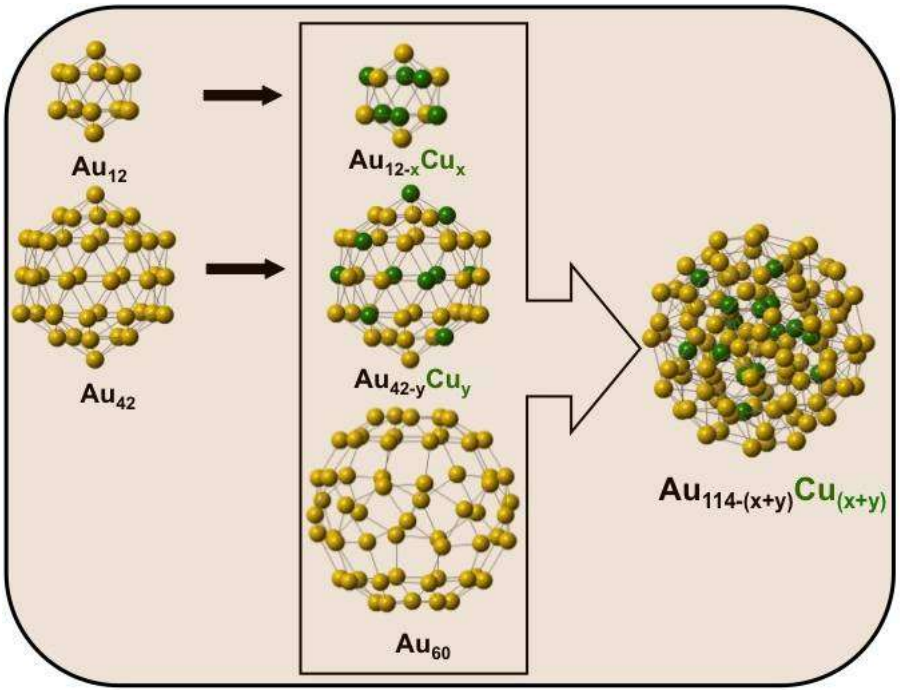

Scheme 1. Proposed location of Cu atoms into $Au_{144}(SR)_{60}$.

The three concentric shells, Au_{12}, Au_{42}, and Au_{60} correspond to $Au_{144}(SR)_{60}$ structure model. The copper (olive) atoms are inter-dispersed into the central 12-atom core, and the surrounding 42-atom shell, so as to maximize the Au-Cu bonds. The atomic radii and surface energy are the other major factors influencing the arrangement of Cu and Au atoms in Au-Cu nanoalloys. The atomic radius of Cu is 1.28 Å and that of Au is 1.44 Å. The smaller atoms will be located at the sterically confined icosahedral core, due to excessive strain.[9] For that reason, Cu atoms incorporated into the $Au_{144}(SR)_{60}$ nanomolecule will favor the central region compared to the surface. The surface energies of Au and Cu are 96.8 and 113.9 meVÅ^{-2} respectively. Due to the

high surface energy of Cu, it tends to occupy the sites in the core, not the surface, to minimize the surface energy of the whole nanomolecule.

Based on these factors, 1) the mixing of Au and Cu atoms is favored due to increased bond strength of Au-Cu bonds. This would maximize the interaction between the two metals; 2) the Cu atoms occupy the core to avoid lattice mismatch due to the difference in the atomic radii; 3) the Cu atoms will occupy the core due to its larger surface energy. The –SR-Au-SR- staple groups must not be affected by Cu atoms due to the high stability of these particles. Therefore, we propose that *Cu atoms are interdispersed into the Au_{12} and Au_{42} cores* so that the number of Au-Cu bonds is maximized. The maximum incorporation of ~23 Cu atoms supports this prediction. This contrasts with the Au-Ag system[19] that incorporates up to 60 Ag atoms, to form $Au_{84}Ag_{60}(SR)_{60}$. Theoretical modeling shows that the 60 Ag atoms are incorporated into the third 60-atom shell.[41]

CONCLUSIONS

In conclusion, a maximum of 23 Cu atoms have been incorporated into the nanomolecule. Cu atoms interdisperse in Au_{12} and Au_{42} shell, the inner most core of $Au_{144}(SR)_{60}$. The doping of Cu atoms changes the composition from gradually from 144-atom to 143-atom and finally into the 145-atom species. We also note that 145-atom species has been observed before.[19,23] This type of effect of doping on the composition of the gold nanomolecules upon alloying is a first report of this kind in thiolated gold alloy nanomolecules. We predict that the compositional changes also affect the atomic structure. The study of atomic structure is beyond the scope of this study and is planned for future. Theoretical calculations[42-44] would provide further insights into electronic structure, atomic structure and ordering.

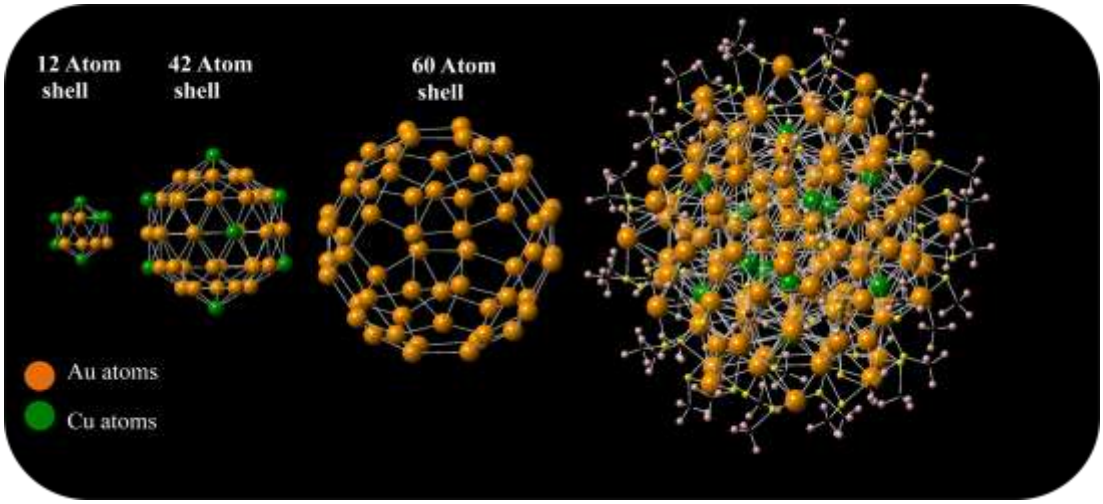

Figure 12. Cu atoms are interdispersed in Au_{12} and Au_{42} shells of $Au_{144}(SR)_{60}$

BIBLIOGRAPHY

(1) Faraday, M. *Philosophical Transactions of the Royal Society of London* **1847**, *147*.

(2) HORIBA SCIENTIFIC.

(3) Merali, Z. In *SMITHSONIAN MAGAZINE* 2013.

(4) Michael W. Heaven, A. D., Peter S. White, Kennedy M. Holt, and Royce W. Murray *J. AM. CHEM. SOC.* **2008**, *130*.

(5) Olga Lopez-Acevedo, J. A., Robert L. Whetten, Henrik Grönbeck, and Hannu Häkkinen *j. phys. Chem. C* **2009**, *113*, 5035.

(6) Yacamán, M. J.; Ascencio, J. A.; Tehuacanero, S.; Marín, M. *Topics in Catalysis* **2002**, *18*, 167.

(7) Ruiz, A.; Arbiol, J.; Cirera, A.; Cornet, A.; Morante, J. R. *Materials Science and Engineering: C* **2002**, *19*, 105.

(8) Chen, K. Z.; Zhang, Z. K.; Cui, Z. L.; Zuo, D. H.; Yang, D. Z. *Nanostructured Materials* **1997**, *8*, 205.

(9) Ferrando, R.; Jellinek, J.; Johnston, R. L. *Chemical reviews* **2008**, *108*, 845.

(10) Wei, W.; Lu, Y.; Chen, W.; Chen, S. *Journal of the American Chemical Society* **2011**, *133*, 2060.

(11) Rice, K. P.; Walker, E. J.; Stoykovich, M. P.; Saunders, A. E. *The Journal of Physical Chemistry C* **2011**, *115*, 1793.

(12) Xu, Z.; Lai, E.; Shao-Horn, Y.; Hamad-Schifferli, K. *Chemical communications* **2012**, *48*, 5626.

(13) Bracey, C. L.; Ellis, P. R.; Hutchings, G. J. *Chemical Society reviews* **2009**, *38*, 2231.

(14) Fields-Zinna, C. A.; Crowe, M. C.; Dass, A.; Weaver, J. E. F.; Murray, R. W. *Langmuir* **2009**, *25*, 7704.

(15) Negishi, Y.; Kurashige, W.; Niihori, Y.; Iwasa, T.; Nobusada, K. *Phys. Chem. Chem. Phys.* **2010**, *12*, 6219.

(16) Xie, S.; Tsunoyama, H.; Kurashige, W.; Negishi, Y.; Tsukuda, T. *ACS Catalysis* **2012**, *2*, 1519.

(17) Negishi, Y.; Iwai, T.; Ide, M. *Chem. Commun.* **2010**, *46*, 4713.

(18) Kumara, C.; Dass, A. *Nanoscale* **2012**, *4*, 4084.

(19) Kumara, C.; Dass, A. *Nanoscale* **2011**, 3064.

(20) Qian, H.; Jiang, D.-e.; Li, G.; Gayathri, C.; Das, A.; Gil, R. R.; Jin, R. *J. Am. Chem. Soc.* **2012**, *134*, 16159.

(21) Kurashige, W.; Munakata, K.; Nobusada, K.; Negishi, Y. *Chemical communications* **2013**, *49*, 5447.

(22) Negishi, Y.; Munakata, K.; Ohgake, W.; Nobusada, K. *The Journal of Physical Chemistry Letters* **2012**, *3*, 2209.

(23) Fields-Zinna, C. A.; Sardar, R.; Beasley, C. A.; Murray, R. W. *J. Am. Chem. Soc.* **2009**, *131*, 16266.

(24) Schaaff, T. G.; Whetten, R. L. *J. Phys. Chem. B* **1999**, *103*, 9394.

(25) Mori, S., Barth, Howard G *Size Exclusion Chromatography*, 1999; Vol. XIV.

(26) Jingjing Li, W. H. a. Y. Y. *Chromatography Method*; CC BY 3.0 license, 2013.

(27) Knoppe, S.; Boudon, J.; Dolamic, I.; Dass, A.; Burgi, T. *Analytical chemistry* **2011**, *83*, 5056.

(28) Tracy, J. B.; Kalyuzhny, G.; Crowe, M. C.; Balasubramanian, R.; Choi, J. P.; Murray, R. W. *J. Am. Chem. Soc.* **2007**, *129*, 6706.

(29) Dass, A.; Stevenson, A.; Dubay, G. R.; Tracy, J. B.; Murray, R. W. *J. Am. Chem. Soc.* **2008**, *130*, 5940.

(30) David B. Pedersen, S. W. *j. Phys. Chem. C* **2007**, *111*, 17493.

(31) Cattaruzza, E.; Battaglin, G.; Gonella, F.; Polloni, R.; Scremin, B. F.; Mattei, G.; Mazzoldi, P.; Sada, C. *Applied Surface Science* **2007**, *254*, 1017.

(32) Darby, S.; Mortimer-Jones, T. V.; Johnston, R. L.; Roberts, C. *The Journal of Chemical Physics* **2002**, *116*, 1536.

(33) Lordeiro, R. A.; Guimarães, F. F.; Belchior, J. C.; Johnston, R. L. *Int. J. Quantum Chem* **2003**, *95*, 112.

(34) Rapallo, A.; Rossi, G.; Ferrando, R.; Fortunelli, A.; Curley, B. C.; Lloyd, L. D.; Tarbuck, G. M.; Johnston, R. L. *The Journal of Chemical Physics* **2005**, *122*, 194308.

(35) Rodrigues, D. D. C.; Nascimento, A. M.; Duarte, H. A.; Belchior, J. C. *Chemical Physics* **2008**, *349*, 91.

(36) Wilson, N. T.; Johnston, R. L. *Journal of Materials Chemistry* **2002**, *12*, 2913.

(37) Jellinek, J.; Krissinel, E. B. *Chemical Physics Letters* **1996**, *258*, 283.

(38) Cerbelaud, M.; Barcaro, G.; Fortunelli, A.; Ferrando, R. *Surface Science* **2012**, *606*, 938.

(39) Hsu, P. J.; Lai, S. K. *J Chem Phys* **2006**, *124*, 044711.

(40) Kerr, J. A. *Chem Rev* **1966**, *66*.

(41) Malola, S.; Häkkinen, H. *J. Phys. Chem. Lett.* **2011**, *2*, 2316.

(42) Pei, Y.; Zeng, X. C. *Nanoscale* **2012**, *4*, 4054.

(43) Hakkinen, H. *Nat Chem* **2012**, *4*, 443.

(44) Aikens, C. M. *J. Phys. Chem. Lett.* **2010**, *2*, 99.

APPENDIX

MALDI TOF-MS Analysis

Monometallic and bimetallic $Au_{144}(SR)_{60}$ nanomolecules capped with Hexanethiol were obtained after a successful synthetic protocol explained in Chapter 2 (Synthetic protocol: Crude product synthesis***)***. The molecular ion peak for $Au_{144}(SC_6H_{13})_{60}$ shows up at 35,397 Da in MALDI TOF-MS. A dotted line has been aligned with the molecular ion peak of the monometallic $Au_{144}(SC_6H_{13})_{60}$,to investigate the compositional effect toward a possible alloying or dealloying. In an event of dealloying of Cu with $Au_{144}(SR)_{60}$, the Cu atoms will bind to the nanomolecule as follow, $Au_{144}Cu_x(SR)_{60}$. For that reason, the overall molecular weight of the dealloyed nanomolecule will increase. Similarly, if the Cu atoms incorporate or alloy with the nanomolecule, the overall molecular weight will decrease as it follows a composition of $Au_{144-x}Cu_x(SR)_{60}$. After obtaining the mass spectral analysis of the complete series of the Au/Cu bimetallic nanomolecules, it was plotted in a graph for further investigation (see Figure.S1). A clear indication of foreign atom incorporation as the molecular ion peak has downshifted from the dotted line. As the precursor ratio is increasing with respect to the Au concentration, the molecular ion peak for each ratio further downshifted. Mass spectrometric data from MALDI TOF-MS is not sufficient to explain the peak broadening at the precursor ratio of Au: Cu-1:0.500. Due to limited information from MALDI TOF-MS analysis, ESI-MS was utilized for a thorough mass spectrometric investigation of Au/Cu bimetallic nanoalloys.

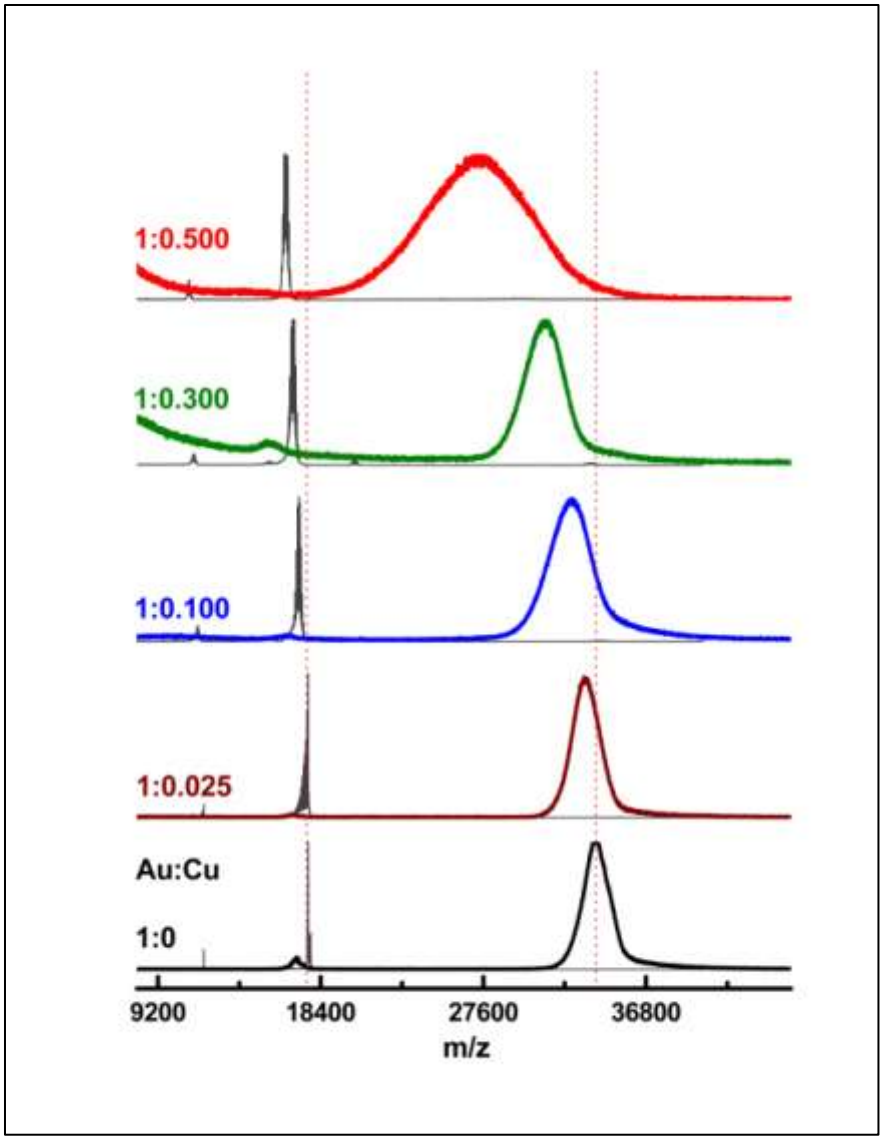

Figure S1. Expanded MALDI TOF-MS of $Au_{144-x}Cu_x(SC_6H_{13})_{60}$ nanomolecules

ESI-MS Analysis

Due to the presence of multiply charged species, the peak resolution observed in ESI-MS is much greater than MALDI TOF-MS. The 2+-charge state had the most abundant species for all the ratios. For that reason, Figure S2 focuses on the 2+-charge state of Au/Cu bimetallic nanomolecules. The m/z value and the molecular ion peak determine the charge state of a nanomolecule. For instance, the molecular ion peak (m) for $Au_{144}(SC_6H_{13})_{60}$ is 35,397 Da. The m/z value for the peak shown in Figure S2 is 17,694 Da. Therefore, the z value equals to the quotient of the molecular ion peak (35,397 Da) and the given m/z value (17,694 Da). Figure S2 illustrates an expansion of the ESI-MS analysis. The atomic mass unit difference between Au and Cu is 133.42 amu. However, in the presence of 2+charge species, the amu difference between Au and Cu is exactly half, 66.7 amu. The first dotted line from right is aligned with the peak corresponding to the monometallic form of $Au_{144}(SC_6H_{13})_{60}$ nanomolecule. Every other dotted line from left to right is corresponding to a single incorporation of a Cu atom into the same nanomolecule, $Au_{144}(SC_6H_{13})_{60}$. The term incorporation can be defined as a replacement of a gold atom in $Au_{144}(SR)_{60}$ with a Cu atom. Since a large atom (Au) is replaced by a smaller atom (Cu), the molecular weight of the bimetallic nanomolecule is reduced from the same amount as the amu difference between Au and Cu, 133.42 Da. As per Figure S2, the difference is 66.7 Da due to the charged state of the species. Since each dotted line represents a single incorporation, the difference between two dotted lines is 66.7 m/z. As illustrated on Au: Cu-1:0.025 series, there are 7 peaks aligning with the dotted line, confirming an incorporation of Cu atoms. After increasing the precursor ratio to 1: 0.1, some intermediate peaks have emerged in

between the dominant Cu atom incorporated peaks, which aligns with the dotted line. The number of Cu atoms in the most intense peak of an envelope represent the average number of Cu atoms present in the species. The tallest peak in ratio 1: 0.1 is corresponding to $Au_{136}Cu_8(SC_6H_{13})_{60}$, with 8 Cu atoms incorporated. When the ratio increased from 1: 0.1 to 1: 0.3, the intermediate peaks from the previous ratio have become dominant. Such changes in the mass spectral analysis indicated another form of bimetallic nanomolecule as the Cu concentration increases. Interestingly, the dominant peaks (ratio 1: 0.3) and the intermediate peaks (ratio 1: 0.1) are located exactly in between two consecutive dotted lines. It suggests that the unknown species present in ratio 1: 0.1 is same as what is present in ratio 1. 0.3. When the ratio increased to 1: 0.5, a new set of peaks emerged. Much broader from the previous peaks and neither aligned with dotted lines nor centered in between them.

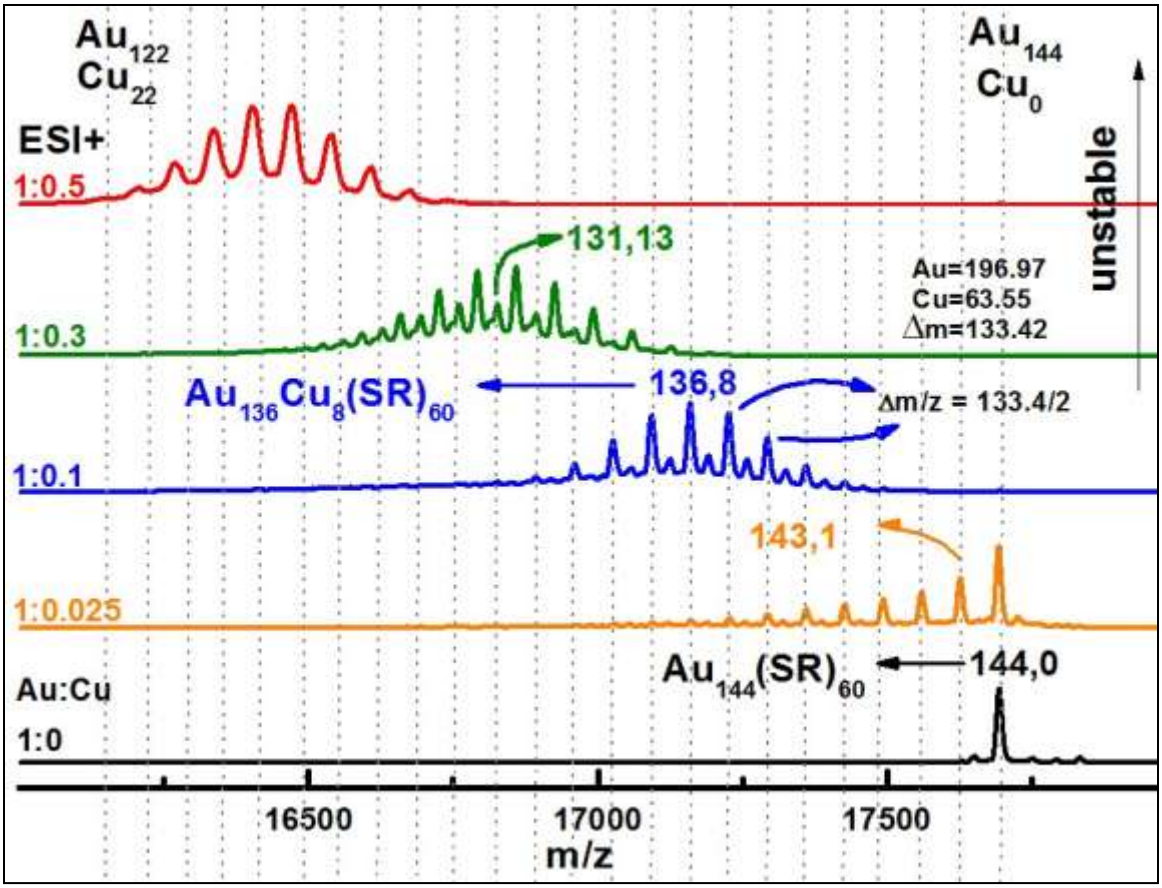

Figure S2. A detailed ESI (2-) mass spectra of $Au_{144-x}Cu_x(SC_6H_{13})_{60}$ nanomolecules

In order to study the effect of Cu incorporation extensively, an expansion of Figure S2 is essential. A thorough peak analysis was performed on each peak to obtain the most accurate metal composition. The number on top of each peak corresponds to the number of Au and Cu atoms in each bimetallic nanomolecule respectively. For instance, the first peak (144, 0) corresponds to the monometallic form of $Au_{144}(SC_6H_{13})_{60}$. The second peak (143, 1) correspond to the bimetallic form of $Au_{143}Cu_1(SC_6H_{13})_{60}$. The presence of three different species was

confirmed after evaluating the metal atom composition of every peak. When comparing the peak distribution with respect to the precursor ratio, the nature of the unknown species can be determined. The peak assignments determined the species as $Au_{144-x}Cu_x(SC_6H_{13})_{60}$, $Au_{143-x}Cu_x(SC_6H_{13})_{61}$, and $Au_{145-x}Cu_x(SC_6H_{13})_{59}$. The control experiment with the initial metal ratio of Au: Cu-1: 0 only contains $Au_{144}(SC_6H_{13})_{60}$. The next ratio, Au: Cu-1: 0.025 shows a few peaks pertaining to the $Au_{144-x}Cu_x(SC_6H_{13})_{60}$. The peak representing the monometallic form of $Au_{144}(SC_6H_{13})_{60}$ is also present in this ratio. The peak set belonging to this ratio ranges from

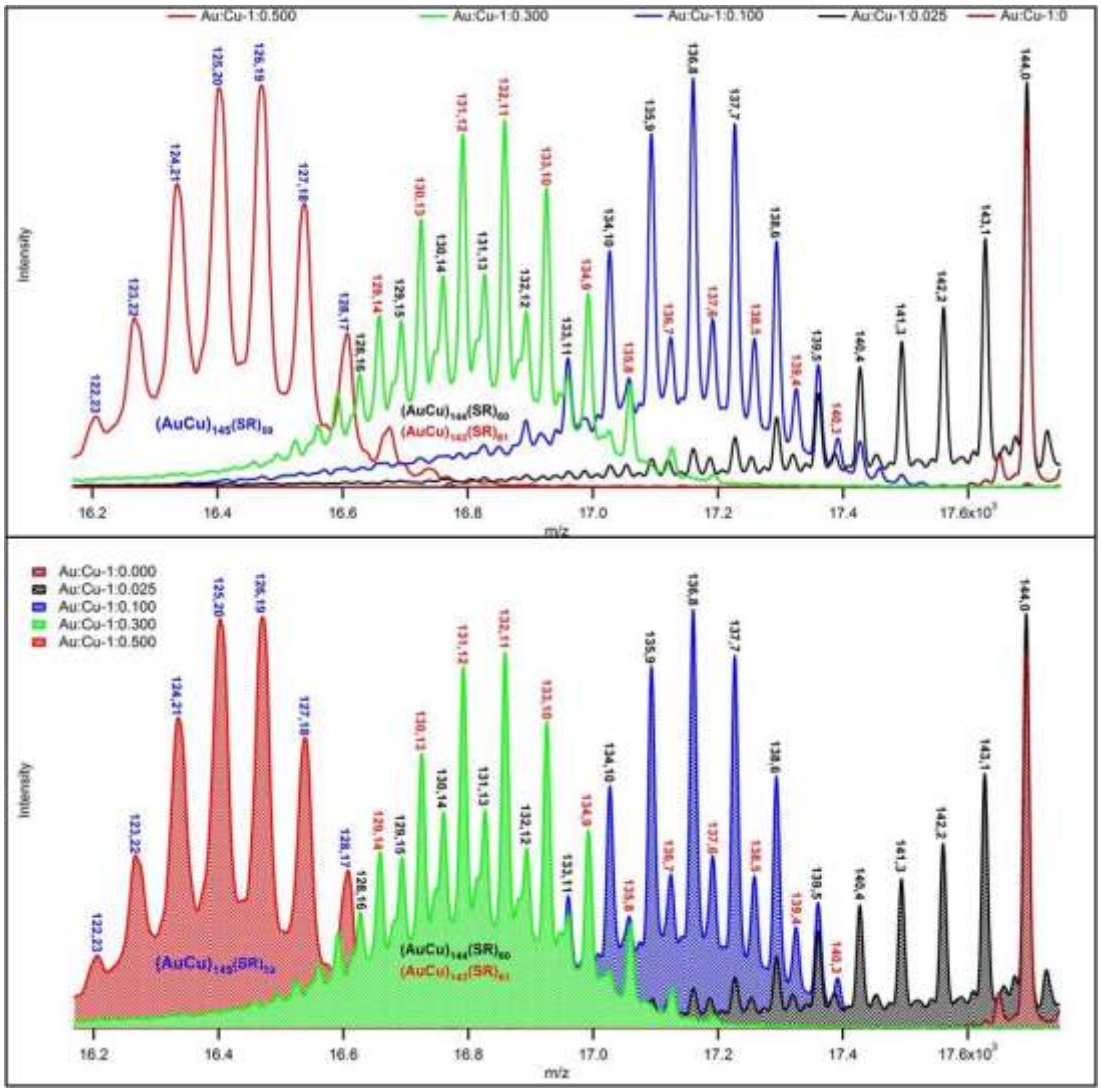

Figure S3. Expanded ESI-MS spectral series of the synthesized $Au_{144-x}Cu_x(SC_6H_{13})_{60}$

Au/Cu [144, 0] to Au/Cu [136, 8]. The precursor ratio of Au: Cu-1: 0.1 mainly consist with peaks belonging to $Au_{144-x}Cu_x(SC_6H_{13})_{60}$. The tallest peak or the average of this peak envelope shows an incorporation of 8 Cu atoms. In this ratio, the emergence of the first set of intermediate peaks can be observed. These intermediate peaks correspond to $Au_{143-x}Cu_x(SC_6H_{13})_{61}$. As the precursor ratio further increased to Au: Cu-1: 0.3, the intermediate peaks from the previous concentration have dominated. The dominant peaks have been assigned as $Au_{143-x}Cu_x(SC_6H_{13})_{61}$. The intermediate peaks of this ratio have been assigned as $Au_{144-x}Cu_x(SC_6H_{13})_{60}$. It is important to address the nature of these intermediate peaks. The intermediate peaks in Au: Cu-1: 0.3, $Au_{144-x}Cu_x(SC_6H_{13})_{60}$ peak envelope has a left shoulder in each peak, possibly an indication of another species. Once the ratio increased to Au: Cu-1: 0.5, the resulting peaks were much broader than the previous precursor concentrations. The peak assignments indicated that in fact $Au_{145-x}Cu_x(SC_6H_{13})_{59}$. The average number of Cu atoms incorporated into this new species is19-20 atoms.

VITA

CURRICULUM VITAE

Asantha Dharmaratne
1731 Anderson Road, Apt#11. Oxford, MS 38655
Email: dharmaratne.asantha@gmail.com
Phone: 662-701-9728

EDUCATION

- M.Sc. in Chemistry, University of Mississippi (GPA-3.46, 2012 – 2015)

  M.Sc. thesis titled "*Effective Tuning of Bimetallic Composition of Gold-Copper Nanomolecules and the Emergence of Plasmon-Like Feature in Optical Spectra*"

- B.Sc. in Chemistry (minor in Mathematics), University of Mississippi (GPA-2.89, 2008-2012)

ACCOMPLISHMENTS

I was able to publish two peer reviewed research articles in a world premiere chemical journal, Journals of the American Chemical Society within the first two years of my undergraduate research at the University of Mississippi.

PEER REVIEWED PUBLICATIONS

1. $Au_{137}(SR)_{56}$ nanomolecules: composition, optical spectroscopy, electrochemistry and electrocatalytic reduction of CO_2. Vijay Reddy Jupally, **Asantha C. Dharmaratne**, David Crasto, Aron J. Huckaba, Chanaka Kumara, Praneeth Reddy Nimmala, Nuwan Kothalawala, Jared H. Delcamp and Amala Dass. *Chem. Commum*., 2014, **50**, 9895-9898.

2. $Au_{144-x}Cu_x(SC_6H_{13})_{60}$ nanomolecules: effect of Cu incorporation on composition and plasmon-like peak emergence in optical spectra. **Asantha C. Dharmaratne** and Amala Dass. *Chem. Commum*., 2014, **50**, 1722-1724.

3. Ligand Exchange Reactions on Au_{38} and Au_{40}Clusters: A Combined Circular Dichroism and Mass Spectrometry Study. Stefan Knoppe, **Asantha C. Dharmaratne**, Ella Schreiner, Amala Dass, Thomas Bürgi. *J.Am. Chem. Soc.* 2010, **132** (47), 16783-16789.

4. Ion Mobility Mass Spectrometry of $Au_{25}(SCH_2CH_2Ph)_{18}$ Nanoclusters. Laurence A. Angel, Lance T. Majors, Asantha C. Dharmaratne, Amala Dass. *ACS Nano* 2010, **4** (8), 4691-4700.

5. Nanocluster Size Evolution Studied by Mass Spectrometry in Room Temperature $Au_{25}(SR)_{18}$ Synthesis. **Asantha. C. Dharmaratne**, T. Krick, A. Dass, *J. Am. Chem. Soc.* 2009, **131**, 13604– 13605.

RESEARCH PRESENTATIONS

1. Effective tuning of bimetallic composition of gold-copper nanomolecules, **Asantha C. Dharmaratne**, Amala Dass. The Graduate School Council research forum held at the University of Mississippi, Oxford, MS (April 28, 2015)

2. Mass spectrometric investigation and atomic ordering of gold copper bimetallic nanomolecules, **Asantha C. Dharmaratne**, Amala Dass. 66th Southeastern Regional Meeting of the American Chemical Society, Nashville, TN. (October 16-19, 2014)

3. Mass Spectrometric and Atomic level Analysis of $Au_{144-x}Cu_x(SR)_{60}$ nanomolecules, **Asantha C. Dharmaratne**, Amala Dass. 247th American Chemical Society National Meeting, Dallas, TX. (March 16-20, 2014)

4. Synthesis and Characterization of Gold/Copper Bimetallic Nanoalloys, **Asantha C. Dharmaratne**, Amala Dass. Mid-South Area Engineering and Sciences Conference, University of Mississippi, Oxford, MS (October 28-29, 2013)

5. Synthesis of $(Au/Cu)_x(SR)_y$ Alloy Nanomolecules, **Asantha C. Dharmaratne**, Amala Dass. 245th American Chemical Society National Meeting, New Orleans, LA. (April 07, 2013)

6. Room Temperature $Au_{25}(SR)_{18}$ Nanocluster Synthesis aided by Size, **Asantha C. Dharmaratne**. 32nd Annual Undergraduate Research Conference, University of Memphis, Memphis, TN. (February 25, 2012)

7. Synthesis and Characterization of Au_{38} Molecular Gold Nanoparticles, Lance Majors, **Asantha C. Dharmaratne**, Amala Dass. 2009 Southeastern Undergraduate Research Conference, University of Alabama, Birmingham. (April 09, 2009)

WORK EXPERIENCE

University of Mississippi
Graduate/ Undergraduate researcher
November 2008 – present

My work as a research student at the University of Mississippi is primarily focused on synthesis and characterization of molecular gold nanoparticles. As a research student, I was responsible for performing scientific chemical analyses and tests on a broad range of samples including mass spectrometric, UV-visible spectroscopic and electrochemical analysis to determine the molecular like characteristics of gold nanoparticles and nanoalloys. The method selections and development for procedures for carrying out assigned analyses to optimize the outcome have been a routine task. Excelled in preparing and maintaining detailed scientific reports identifying samples. Routine maintenance and regular troubleshooting of sophisticated mass spectrometers. Expertise in scientific instruments and computer systems in the laboratory to analyze and identify/ characterize samples. The scientific instruments include Matrix Assisted Laser Desorption Ionization Time of Flight mass spectrometry (MALDI TOF-MS), Electrospray Ionization Mass Spectrometry (ESI-MS), Gas Chromatography Mass Spectrometry (GCMS), Liquid Chromatography Mass Spectrometry (LCMS), Inductively Coupled Plasma Mass Spectrometry (ICP-MS), Fourier Transform Infrared (FTIR) and Ultra Violet-visible (UV-vis) Spectroscopy, X-Ray Diffraction, Microscopy (SEM/ TEM), and High Performance Liquid Chromatography Mass Spectrometry (HPLC-MS), Size Exclusion Chromatography (SEC). Expertise with computer software and statistical analysis and critical interpretation of results.

University of Mississippi
Undergraduate/ Graduate teaching assistant
May 2012-present

My duties as a Teaching Assistant at the Organic Chemistry Division in the Department of Chemistry and Biochemistry is mentoring undergraduate students and assess their performances in lab activities. Guiding them with assigned laboratory experiments and perform scientific

chemical analyses and tests to identify given samples using methods such as gas chromatography, and Fourier transform infrared spectroscopy analyses. Quantitative Analysis laboratory method validation using HPLC techniques in experiments such as determination of Caffeine content in commercially available chocolate. Enforce firm safety protocols to maintain good laboratory practice regulations during the lab session and I make recommendations for strict monitoring and enforcing purposes when handling hazardous chemicals during laboratory sessions are in progress.

University of Peradeniya (Sri Lanka)
Pre-University volunteered research assistant
August 2007 – January 2008

My area of interest as a pre-University volunteered research assistant was modified clays and clay-polymer nanocomposites. I was able to develop a method to encapsulate urea within inter layers of montmorillonote particles, and studied the leaching kinetics to improve the slow release of urea within inter layers of montmorillonote particles. Such method selections and developments have a higher potential in the Agricultural sector as an essential/ profitable fertilizer.

HONORS AND AWARDS

- Second place - Blueprint Mississippi Social Business Challenge, which asks students to develop and present business plans to solve one of Mississippi's pressing social problems organized by the McLean Institute for Public Service and Community Engagement and the School of Business Administration at the University of Mississippi (November, 2014)

- Included in the 2011-2012 Who's Who Among Students in American Universities and Colleges, in recognition of those students who have made significant contributions to their campus in the areas of scholarship, leadership, and student activities

- Best Undergraduate Student Researcher of the Year 2010-2011, by local section of the American Chemical Society and the Department of Chemistry and Biochemistry, University of Mississippi

VOLUNTEER WORK AND COMMUNITY INVOLVEMENT

- Regional and Mississippi state Science Fair judge - (2013- present)
- Student Note Taker (Student Disability Service, University of Mississippi)
- Active participant - Jean Jones Cancer Run (2009- present)

EXTRA CURRICULAR ACTIVITIES

- University of Mississippi- Cricket Team (2008- present)
- Black Belt Degree in Kickboxing- World Martial Arts Association-2008

PROFESSIONAL ORGANIZATIONS

- American Chemical Society